Biosensors and Bioelectronics 43 (2013) 226–230

Contents lists available at SciVerse ScienceDirect

Biosensors and Bioelectronics

journal homepage: www.elsevier.com/locate/bios

Short communication

# A single mesoporous ZnO/Chitosan hybrid nanostructure for a novel free nanoprobe type biosensor

Minggang Zhao [a], Jingyun Huang [a,b,*], Yu Zhou [a], Qi Chen [a], Xinhua Pan [a], Haiping He [a], Zhizhen Ye [a,b,*]

[a] Department of Materials Science and Engineering, State Key Laboratory of Silicon Materials, Zhejiang University, Hangzhou 310027, China
[b] Cyrus Tang Center for Sensor Materials and Applications, Zhejiang University Hangzhou 310058, China

ARTICLE INFO

*Article history:*
Received 10 October 2012
Received in revised form
22 November 2012
Accepted 30 November 2012
Available online 20 December 2012

*Keywords:*
Single mesoporous ZnO
Inorganic–organic
Hybrid
Free probe
Biosensor

ABSTRACT

A novel method of fabricating a free probe type nanoscale biosensor is first demonstrated. A free probe type biosensor based on a single one-dimensional (1D) mesoporous ZnO/Chitosan inorganic–organic hybrid nanostructure is constructed. The as-prepared biosensor exhibited excellent biosensing performance and was stable in solution due to its inorganic–organic hybrid structure. The special mesoporous nanostructure with protuberances favors enzymes loading and enhances electrical communication efficiency. The feasibility of employing a single 1D nanostructure as a separate free nanoprobe for biosensing is demonstrated. This kind of free probe type biosensor will not only provides a new tool for micro-targets detection in microcell and enzymatic studies, but also has the potential to be inserted into single cell or other microorganism for biological studies.



## 1. Introduction

Miniaturization of devices and trace detection are important pursued objectives of biosensors. Exploiting nanoscale biosensors, especially the single 1D nanostructure based biosensors, may allow innovative physiological and biological applications by means of probing local cellular environments (Heller et al., 2005; Vo-Dinh et al., 2006). Moreover, advances on nanoscale biosensors may open the route toward electrochemical single-biomolecular studies (Besteman et al., 2003; Obataya et al., 2005). Nanomaterials have unique advantages in application of biosensors, including high specific surface area for high enzyme loading, desirable microenvironment for retaining enzymatic bioactivity, nanoscale for ultra-miniature devices, and unique optical and electrical properties (Xiao et al., 2003; Xu et al., 2006; Ahmad et al., 2010; Xie et al., 2012; Cohen-Karni et al., 2012; Heller et al., 2009; Star et al., 2003; Fan et al., 2005; Yeh et al., 2009; Wei et al., 2010). Micro-devices based on single 1D nanomaterials, such as Si nanowire (Gao et al., 2011; Stern et al., 2007; Tian et al., 2010; Gao et al., 2012) and C nanotube (Besteman et al., 2003; Heller et al., 2009), have been fabricated and exhibited good detection ability. Because of the need of probing local cellular environments and single-biomolecular studies, it is essential to exploit a single 1D nanostructure based free probe type biosensor. From previous reports, the single nanomaterial based biosensors were widely fabricated as field effect transistors (FETs). However, the single nanostructure is limited to be used as a free probe for microbial monomer in-vivo detection and other applications, due to the connected electrode construction and more complicated and precise fabricating technics are required. Here, a novel method of fabricating a single 1D nanostructure based free probe type nanoscale biosensor is demonstrated.

The hybridization of two materials could lead to an improvement and/or a combination of intrinsic properties of each single-component counterpart (Anyaogu et al., 2008; Hirai et al., 2000; Qi et al., 2001). ZnO nanostructures are promising for biosensors, due to their high-specific surface area, high electron communication features, non-toxicity, biocompatibility and high isoelectric point (IEP∼9.5) (Gu et al., 2009; Yang et al., 2009; Yang et al., 2010; Li et al., 2008). In particular, the high IEP of ZnO makes it suitable for absorption of proteins with low IEPs by electrostatic interactions with high binding stability (Topoglidis et al., 2005; Usman et al., 2009; Wang et al., 2006), such as glucose oxidase (GOx) (IEP∼4.5), DNA. The additional benefit of ZnO nanostructures is an oxide semiconductor with good stability in air environment, as compared to that of non-oxide semiconductors (Kim et al., 2006). For many non-oxide semiconductor nanomaterials, the formed insulating native oxide layer may degrade device reliability and sensitivity (Zhou et al., 2003). Various ZnO

* Corresponding authors at: Department of Materials Science and Engineering, State Key Laboratory of Silicon Materials, Zhejiang University, Hangzhou 310027, China. Tel.: +86 571 879 521 18; fax: +86 571 879 526 25.
*E-mail addresses:* huangjy@zju.edu.cn (J. Huang), yezz@zju.edu.cn (Z. Ye).

0956-5663/$ - see front matter © 2012 Elsevier B.V. All rights reserved.
http://dx.doi.org/10.1016/j.bios.2012.11.041

nanostructure based biosensors have been fabricated to detect uric acid, glucose, protein, biological molecules and so on, and good performances were achieved (Kim et al., 2006; Wang et al., 2010; Llegbusi et al., 2010; Yang et al., 2009; Zhang et al., 2004). Chitosan (CHIT) is a biodegradable natural biopolymer, which can be mostly found in crustacean shells. It has been widely used for immobilization of enzymes, due to its biodegradability, chemical inertness, nontoxicity, biocompatibility, high mechanical strength, good film-forming properties, and low cost. Here, the inorganic–organic hybrid leads to a combination of large specific surfaces, high electrical communication of mesoporous ZnO and excellent film-forming, enzyme immobilization ability of organic CHIT.

Immobilization of biomolecules in tailor-made nanometer scale structures can significantly improve the performance of biocatalysis processes. Mesoporous materials with well-controlled pore structures can afford high loading and long-term stability of biocatalysts, as well as low mass-transfer resistance (Kyotani, 2000; Li and Jaroniec, 2001; Johnson et al., 1999; Lee et al., 2005).

Herein, a novel free probe type nanoscale biosensor fabricated by a single mesoporous ZnO/CHIT hybrid nanostructure is first demonstrated. A separate single electrode construction different from that of FET permits its use independently as a free probe. The single mesoporous inorganic–organic hybrid nanostructure exhibited excellent biosensing performance and stability. The feature of mesoporous structure with pores and protuberances for immobilizing GOx enzymes was studied. It can not only afford high loading and long-term stability of enzymes, but also high electrical communication efficiency. Furthermore, this biosensor has the potential to be developed as a single nanoprobe for intra cellular detection and will provide a powerful tool for biological studies.

## 2. Materials and methods

### 2.1. Chemicals and reagents

Glucose oxidase (100–250 U/mg) was purchased from Sigma. Chitosan (deacetylation value $\geq 95\%$) was purchased from Aladdin-reagent. Zinc acetate ($Zn(CH_3COO)_2 \cdot 2H_2O$), sodium dihydrogen phosphate ($NaH_2PO_4 \cdot 2H_2O$), disodium hydrogen phosphate ($Na_2HPO_4 \cdot 12H_2O$), acetic acid ($CH_3COOH$) and anhydrous ethanol ($C_2H_5OH$) were purchased from Shanghai Hushi-reagent and all of them were analytically pure. Polyvinyl alcohol (polymerization $1750 \pm 50$) was purchased from Tianjin Shengao-reagent.

### 2.2. Preparation of single mesoporous ZnO nanostructure and electrode

A substrate electrode was prepared first, including a silicon wafer with a 500 nm thermally grown oxide and a 100 nm gold layer deposited by electron-beam evaporation. In a typical procedure, a polyvinyl alcohol (PVA) sol solution (7 wt%) was prepared through water bath at 85 °C first, and then zinc acetate (2.19 g) was added into 30 ml as-prepared PVA solution with stirring and heating; during this time 2 ml alcohol was added dropwise into the solution. The viscous precursor sol solution was ready for electrospinning after aging. A single mesoporous ZnO nanofiber prepared by electrospining and sequent annealing process was placed on the substrate electrode. Then a part of Au layer was encapsulated in polymethyl methacrylate (PMMA) to avoid the leaky current. A schematic illustration of biosensor construction is shown in Fig. 1a.

### 2.3. Immobilization of enzymes

The GOx enzymes were successfully immobilized in the mesoporous ZnO nanofibers by electrostatic adsorption interaction (Wei et al., 2006) and CHIT-assisted cross-linking technique (Xu et al., 2006). Firstly, GOx enzymes solution (10.0 mg/ml) was prepared by dissolving GOx in 0.01 M phosphate buffer saline (PBS pH 7.4), and 0.5 wt% CHIT (molar weight $\sim 1 \times 10^6$, 75–85% deacetylation) solution was prepared by dissolving CHIT in acetic acid solution. Then, a single ZnO nanofiber was dipped in GOx solution and left for 15 min. After dried in air, the CHIT solution was further applied onto the electrode surface to prevent possible enzyme leakage. Then the device was dried at 4 °C overnight in a refrigerator, followed by washing step to remove the unimmobilized GOx.

### 2.4. Apparatus and measurements

The morphology and size of as-synthesized samples were characterized with SU-70 scanning electron microscopy (SEM). All the electrochemical experiments were performed with a WPG100e electrochemical workstation (Korea). All electrical measurements were carried out in aqueous solutions (PBS pH = 7.4) at room temperature. The single ZnO/GOx/CHIT hybrid nanostructure was used as a working electrode.

## 3. Results and discussion

### 3.1. Characterization of the biosensor

Fig. 1b and c shows the SEM images of the ZnO nanofiber before and after the immobilization of GOx, respectively. For the single ZnO nanofiber before immobilization of GOx shown in Fig. 1b the diameter is 250 nm and the surface is rough with lots of pores. After immobilization of GOx, the surface morphology of nanofiber changed by being modified with a layer of GOx and CHIT. As shown in Fig. 1c, we can see that the pores were embedded and diameter was about 50 nm larger after coating with an integrated nanosheath. For a clear presentation of the immobilization process of GOx, the detailed structure of mesoporous ZnO nanofiber in different stages of the enzymes immobilization process is observed from a higher resolution SEM image, as shown in Fig. 2. Before GOx immobilization, the surface of mesoporous ZnO nanofiber is rough. As is shown in Fig. 2a, a variety of protuberances and pores with sizes from 4 to 50 nm are distributed in the nanofiber. The mesoporous structures can afford high enzymes loading without serious mass-transfer limitations and result in high catalytsis efficiency (Lee et al., 2005). In addition, the special structure can afford favorable environment for immobilization of GOx molecules, which is just like the natural coral reefs being favorable for the living of coral polyps. After electrostatic adsorption of GOx molecules, the surface morphology of nanofiber is changed. As is shown in Fig. 2b, the surface of mesoporous ZnO is distributed with GOx molecules with diameters of 10–20 nm, which is in agreement with the reported dimension of GOx molecules (Chi et al., 1994). Uniform and orderly distribution of enzyme molecules signified an electrostatic self-assembly process, rather than a messy stacked process. Pores are embedded and protuberances are coated with GOx molecules. For more stable immobilization and preventing the leakage of GOx molecules, the organic permeable CHIT was applied onto the surface of ZnO nanofiber. Due to its excellent film formation, adhesion ability and biocompatibility, CHIT is favorable for enzyme immobilization. The CHIT modified ZnO/GOx nanostructure is shown in Fig. 2c; it is observed that the surface is coated with a CHIT shell compared to Fig. 2b. Abundant works have

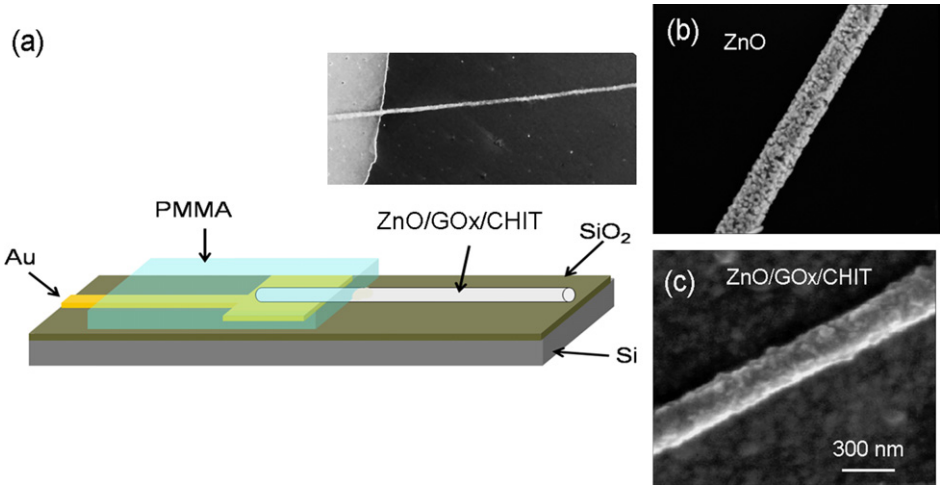


**Fig. 1.** Construction of the biosensor. (a) Schematic picture of the single ZnO/CHIT nanostructure based biosensor. The inset shows the SEM images of a single ZnO nanofiber grown on the $SiO_2$ layer and Au leads. (b) SEM image of the single ZnO nanofiber before immobilization of GOx. (c) SEM image of the same single ZnO nanofiber after immobilization of GOx.

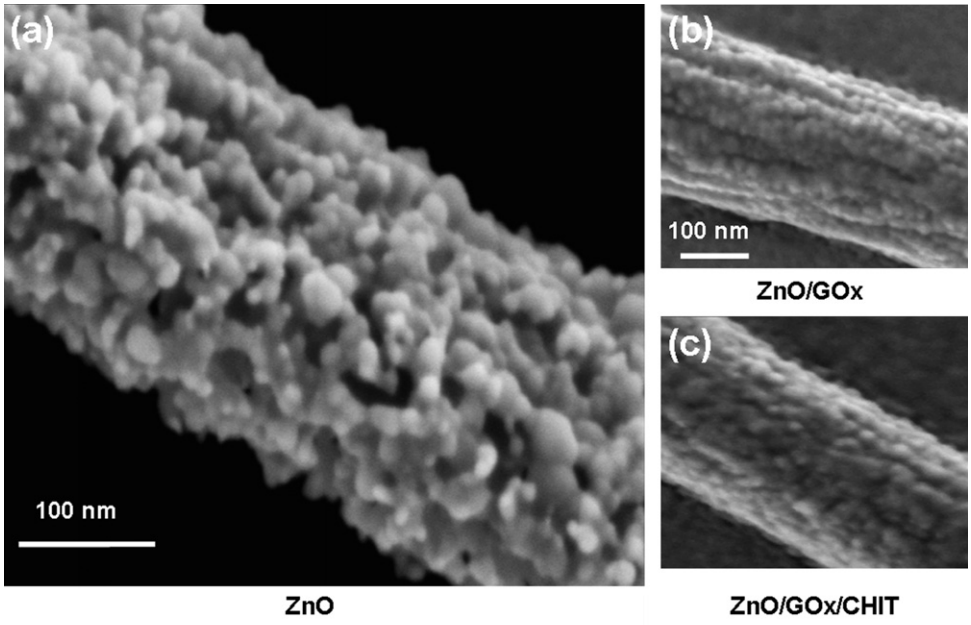


**Fig. 2.** Redox enzymes GOx immobilization process. (a) High resolution SEM images of specific morphology and structure of the ZnO nanofiber with pores and protuberances. (b) Specific morphology and structure of the ZnO nanofiber after loading with GOx molecules. (c) Final SEM images of the ZnO nanofiber after coating with CHIT.

demonstrated that the CHIT modified ZnO biosensor exhibited high stability in biological fluids of various pH (Solanki et al., 2008; Wang et al., 2006; Narang, Pundir, 2011; Yang et al., 2012; Liu et al., 2008). Therefore, the CHIT shell here is important for the stability of biosensor in solution. A schematic illustration of GOx immobilization process is shown in Supplementary data (Fig. S1).

### 3.2. Application as a glucose biosening nanoprobe

Electrochemical behavior of the biosensor is described in Supplementary data (Fig. S2). The single mesoporous ZnO/GOx/CHIT hybrid nanostructure appears to be sensitive to glucose. Fig. 3 shows the real-time measurements where the current of biosensor in PBS has been recorded as a function of time. When water was added to the liquid (red arrow), no significant change in current was observed. When glucose was added to the liquid (blue arrow), however, the current of biosensor increased by about 80%. The response time is as short as 3 s, so fast response can be observed in Fig. 3b as well. This indicates a good electrocatalytic oxidative and fast electron exchange behavior of the biosensor, due to the special surface structure for higher enzyme loading and compatible microenvironment to help the enzyme to retain its bioactivity. The corresponding calibration curve of current versus glucose concentration is shown in Fig. 3c. It is found that the current increases with the increasing glucose concentration at a large linear slope from 0.2 to 12 mM (correction coefficient $R=0.998$). The stability of biosensor is shown in Fig. 3d. As revealed in the inset illustration, the electrical signals of biosensor in the solutions were quite stable for more than 60 min in our experiments. The long-term stability of enzyme electrode was evaluated by measuring its performance every few days. It can be seen that the biosensor retained around 85% of

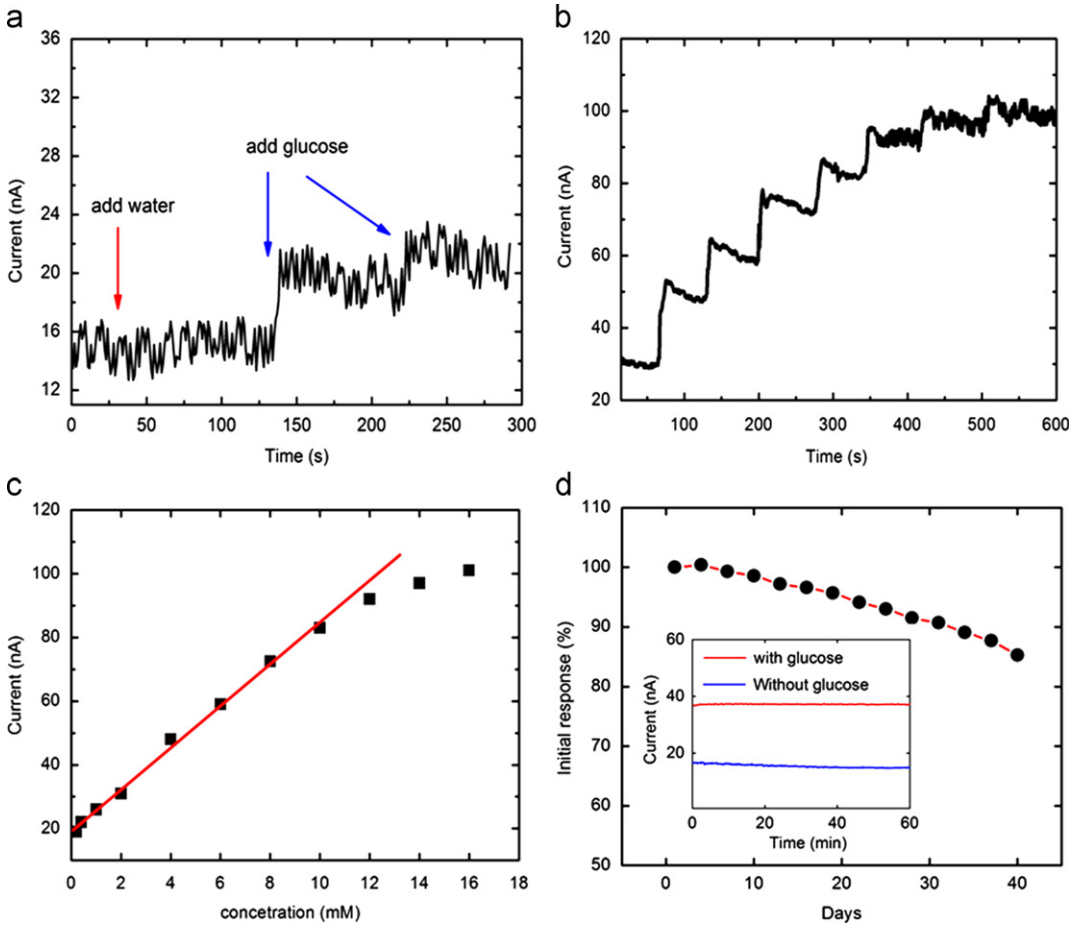


**Fig. 3.** Real time electronic response of biosensor to glucose. The current is measured as a function of time in PBS. The applied voltage is 500 mV. (a) Real time response of the single ZnO/CHIT composite nanostructure with added water and glucose. After deionized water (red arrow) was added to the liquid, no current increase was found. However, after glucose (blue arrow) was added, the current increased rapidly. (b) Real time response of the single ZnO/CHIT composite nanostructure with added 2 mM glucose into the liquid step by step; stepwise current increase was seen. (c) Calibration curve of glucose concentration versus current; a large linear slope from 0.2 to 12 mM was observed. (d) Stability of biosensor by continuous measurement in minutes and regularly checking in days. (For interpretation of the references to color in this figure, the reader is referred to the web version of this article.)

initial response after 40 days, indicating that the immobilized GOx efficiently retained its bioactivity for a quite long time. These results prove that mesoporous ZnO/CHIT hybrid nanostructure used as a matrix provides a good environment for the enzyme activity. The selective detection of glucose in real solutions (cell lysate) is shown in Fig. S3. The addition of these potential interferents (ascorbic acid and uric acid) did not substantially change the signal. The results demonstrated that the biosensor could be used for glucose detection in real solutions (the relative standard deviation was less than 5%).

The working mechanism of biosensor is schematically illustrated in Fig. S4, as described in Wang (2008). On the basis of this working mechanism, the potential possibility of applying a single nanostructure for in-vivo measurements of microbial monomer is schematically illustrated in Fig. S4c. Further experiments are needed to unambiguously identify the feasibility of microbial monomer research.

It is well known that the active center of flavin adenine dinucleotide (FAD) of GOx is deeply buried in a protein shell, which forms a barrier to efficient electrical communication between the redox center of GOx and solid electrode surfaces (Fig. S5a, b). Previous reports have demonstrated that nanostructures with the scale close to enzyme molecules were able to penetrate the protein and got close to the redox center due to the small size (Xiao et al., 2003; Guiseppi-Elie and Lei, 2002; Gooding et al., 2003; Liu et al., 2005). An efficient pathway was thus provided for electrons transferring from a redox enzyme to the underlying electrode. In this study, the fast response of biosensor is attributed to the enhanced electrical communication of special structure with protuberances, as shown in Fig. S5c. Various secondary protuberances with the scale several to a dozen nanometers close to GOx molecules are observed. The small scale makes them able to penetrate the protein shell and get close to the redox center of FAD of GOx molecules by electrostatic adsorption. Moreover, the vertical structure is helpful for to refold GOx molecules. Therefore the protuberances in mesoporous ZnO may help enhancing the electrical communication efficiency and result in fast response.

## 4. Conclusions

In conclusion, we demonstrated a novel free probe type nanoscale biosensor based on a single mesoporous ZnO/CHIT hybrid nanostructure. The biosensor exhibited excellent biosensing performance with high sensitivity and fast response. The characteristic structure of mesoporous ZnO with pores and protuberances was favorable for enzymes loading and enhancing the electrical communication efficiency. The wrapped CHIT shell played an important role in stable immobilization of enzymes and stability of the biosensor. The free probe construction indicates that the single ZnO/CHIT hybrid nanostructure has the potential

to be further developed as a nanoprobe for trace detection in microcell and microbial monomer in in-vivo research. This fabricating strategy can be extended to other 1D nanomaterials.

## Acknowledgments

This work was partly supported by the National Natural Science Foundation of China and the Doctorate Fund of the Ministry of Education.

## Appendix A. Supporting information

Supplementary data associated with this article can be found in the online version at http://dx.doi.org/10.1016/j.bios.2012.11.041.

## References

Ahmad, M., Pan, C.F., Luo, Z.X., Zhu, J., 2010. Journal of Physical Chemistry C 114, 9308–9313.
Anyaogu, K.C., Cai, X., Neckers, D.C., 2008. Macromolecules 41, 9000–9003.
Besteman, K., Lee, J.O., Wiertz, F.G.M., Heering, H.A., Dekker, C., 2003. Nano Letters 3, 727–730.
Chi, Q.J., Zhang, J.D., Dong, S.J., Wang, E.K., 1994. Journal of the Chemical Society, Faraday Transactions 90 (14), 2057–2060.
Cohen-Karni, T., Casanova, D., Cahoon, J.F., Qing, Q., Bell, D.C., Lieber, C.M., 2012. Nano Letters 12, 2639–2644.
Fan, R., Karnik, R., Yue, M., Li, D.Y., Majumdar, A., Yang, P.D., 2005. Nano Letters 5, 1633–1637.
Gao, A.R., Lu, N., Dai, P.F., Li, T., Pei, H., Gao, X.L., et al., 2011. Nano Letters 11, 3974–3978.
Gao, R.X., Strehle, S., Tian, B.Z., Cohen-Karni, T., Xie, P., Duan, X.J., Qing, Q., Lieber, C.M., 2012. Nano Letters 12, 3329–3333.
Gooding, J.J., Wibowo, R., Liu, J.Q., Yang, W., Losic, D., Orbons, S., Mearns, F.J., Shapter, J.G., Hibbert, D.B., 2003. Journal of the American Chemical Society 125, 9006–9007.
Gu, B.X., Xu, C.X., Zhu, G.P., Liu, S.Q., Chen, L.Y., Wang, M.L., et al., 2009. Journal of Physical Chemistry B 113, 6553–6557.
Guiseppi-Elie, A., Lei, C.H., 2002. Nanotech 13, 559.
Heller, I., Kong, J., Heering, H.A., Williams, K.A., Lemay, S.G., Dekker, C., 2005. Nano Letters 5, 137–142.
Heller, I., Mannik, J., Lemay, S.G., Dekker, C., 2009. Nano Letters 1, 377–382.
Hirai, T., Saito, T., Komasawa, I., 2000. Journal of Physical Chemistry B 104, 11639.
Johnson, S.A., Ollivier, P.J., Mallouk, T.E., 1999. Science 283, 963–965.
Kim, J.S., Park, W.L., Lee, C.H., Yi, G.C., 2006. Journal of the Korean Physical Society 49, 1635–1639.
Kyotani T., 2000. Carbon 38, 269.
Lee, D., Lee, J., Kim, J., Na, H.B., Kim, B., et al., 2005. Advanced Materials 17, 2828–2833.
Liu, J.Q., Chou, A., Rahmat, W., Paddon-Row Michael, N., Gooding, J.J., 2005. Electroanalysis 17, 38–46.
Li, Z.J., Jaroniec, M., 2001. Journal of the American Chemical Society 123, 9208–9209.
Liu, Z.M., Liu, Y.L., Shen, G.L., Yu, R.Q., 2008. Analytical Letters 41 (6), 1083–1095.
Li, Z., Yang, R.S., Yu, M., Bai, F., Li, C., Wang, Z.L., 2008. Journal of Physical Chemistry C 112, 20114–20117.
Llegbusi, O.J., Song, H.W., Chakrabarti, R., 2010. Journal of Bionic Engineering 7, S30–S35.
Narang, J., Pundir, C.S., 2011. International Journal of Biological Macromolecules 49, 707–715.
Obataya, I., Nakamura, C., Han, S., Nakamura, N., Miyake, J., 2005. Nano Letters 5, 27–30.
Qi, L., Co1lfen, H., Antonietti, M., 2001. Nano Letters 1, 61–65.
Solanki, P.R., Kaushik, A., Ansari, A.A., Sumana, G., Malhotra, B.D., 2008. Applied Physics Letters 93, 163903.
Star, A., Gabriel, J.P., Bradley, K., Gruner, G., 2003. Nano Letters 3, 459–463.
Stern, E., Klemic, J.F., Routenberg, D.A., Wyrembak, P.N., Turner-Evans, D.B., Hamilton, A.D., et al., 2007. Nature 445, 519–522.
Tian, B.Z., Cohen-Karni, T., Qing, Q., Duan, X.J., Xie, P., Lieber, C.M., 2010. Science 329, 830–834.
Topoglidis, E., Palomares, E., Astuti, Y., Green, A., Campbell, C.J., Durrant, J.R., 2005. Elec Anal 17, 1035.
Usman Ali, S.M., Nur., O., Willander, M., Danielsson, B., 2009. IEEE Tran. Nanotech 8, 678–683.
Vo-Dinh, T., Kasili, P., Wabuyele, M., 2006. Nanomedicine: Nanotechnol 2, 22–30.
Wang, J., 2008. Chemical Reviews 108, 814–825.
Wang, L.Y., Sun, Y., Wang, J., Wang, J., Yu, A.M., Zhang, H.Q., et al., 2010. Journal of Colloid and Interface Science 351, 392–397.
Wang, Z.J., Yang, Y.H., Li, J.S., Gong, J.L., Shen, G.L., Yu, R.Q., 2006. Talanta 69, 686–690.
Wei, A., Sun, X.W., Wang, J.X., Lei, Y., Cai, X.P., Li, C.M., Dong, Z.L., Huang, W., 2006. Applied Physics Letters 89, 123902.
Wei, Y.Y., Li, Y., Liu, X.Q., Xian, Y.Z., Shi, G.Y., Jin, L.T., 2010. Biosensors & Bioelectronics 26, 275–278.
Xiao, Y., Patolsky, F., Katz, E., Hainfeld, F., Willner, I., 2003. Science 299, 1877–1881.
Xie, P., Xiong, Q., Fang, Y., Qing, Q., Lieber, C.M., 2012. Nature Nanotech 7, 119–125.
Xu, Q., Mao, C., Liu, N.N., Zhu, J.J., Sheng, J., 2006. Biosensors & Bioelectronics 22, 768–773.
Yang, K., She, G.W., Wang, H., Ou, X.M., Zhang, X.H., Lee, C.S., Lee, S.T., 2009. Journal of Physical Chemistry C 113, 20169–20172.
Yang, L.J., Xiong, H.Y., Zhang, X.H., Wang, S.F., 2012. Bioelectrochemistry 84, 44–48.
Yang, L.Q., Ren, X.L., Tang, F.Q., Zhang, L., 2009. Biosensors & Bioelectronics 25, 889–895.
Yang, Z., Zong, X.L., Ye, Z.Z., Zhao, B.H., Wang, Q.L., Wang, P., 2010. Biomaterials 31, 7534–7541.
Yeh, P.H., Li, Z., Wang, Z.L., 2009. Advanced Materials 21, 4975–4978.
Zhang, F.F., Wang, X.L., Ai, S.Y., Sun, Z.D., Wan, Q., Zhu, Z.Q., et al., 2004. Analytica Chimica Acta 519, 155–160.
Zhou, X.T., Hu, J.Q., Li, C.P., Ma, D., Lee, C.S., Lee, S.T., 2003. Chemical Physics Letters 369, 220–224.